JACS
JOURNAL OF THE AMERICAN CHEMICAL SOCIETY
Cite This: J. Am. Chem. Soc. XXXX, XXX, XXX−XXX
Communication
pubs.acs.org/JACS

Atomically Dispersed Pd on Nanodiamond/Graphene Hybrid for Selective Hydrogenation of Acetylene

Fei Huang,[†,‡,#] Yuchen Deng,[§,#] Yunlei Chen,[∥,⊥,#] Xiangbin Cai,[+,#] Mi Peng,[§] Zhimin Jia,[†,‡] Pengju Ren,[∥,¶] Dequan Xiao,[⊗] Xiaodong Wen,[∥,¶] Ning Wang,[+] Hongyang Liu,*[,†] and Ding Ma*[,§]

[†]Shenyang National Laboratory for Materials Science, Institute of Metal Research, Chinese Academy of Sciences, Shenyang 110016, People's Republic of China

[‡]School of Materials Science and Engineering, University of Science and Technology of China, Hefei 230026, People's Republic of China

[§]Beijing National Laboratory for Molecular Engineering, College of Chemistry and Molecular Engineering and College of Engineering, BIC-ESAT, Peking University, Beijing 100871, People's Republic of China

[∥]State Key Laboratory of Coal Conversion, Institute Coal Chemistry, Chinese Academy of Sciences, Taiyuan 030001, People's Republic of China

[⊥]University of Chinese Academy of Science, No. 19A Yuanquan Road, Beijing 100049, People's Republic of China

[+]Department of Physics, Hong Kong University of Science and Technology, Clear Water Bay, Kowloon, Hong Kong SAR, People's Republic of China

[¶]National Energy Center For Coal to Clean Fuel, Synfuels China Co., Ltd, Huairou District, Beijing 101400, People's Republic of China

[⊗]Center for Integrative Materials Discovery, Department of Chemistry and Chemical Engineering, University of New Haven, 300 Boston Post Road, West Haven, Connecticut 06516, United States

Supporting Information

ABSTRACT: We reported here a strategy to use a defective nanodiamond-graphene (ND@G) to prepare an atomically dispersed metal catalyst, i.e., in the current case atomically dispersed palladium catalyst which is used for selective hydrogenation of acetylene in the presence of abundant ethylene. The catalyst exhibits remarkable performance for the selective conversion of acetylene to ethylene: high conversion (100%), ethylene selectivity (90%), and good stability. The unique structure of the catalyst (i.e., atomically dispersion of Pd atoms on graphene through Pd−C bond anchoring) blocks the formation of unselective subsurface hydrogen species and ensures the facile desorption of ethylene against the overhydrogenation to undesired ethane, which is the key for the outstanding selectivity of the catalyst.

Ethylene, produced from the petroleum industry, is an important raw material for the production of polyethylene. However, a trace amount of acetylene (~1%) is usually present in the ethylene feed, which would poison the catalysts used for ethylene polymerization and reduce the quality of polyethylene.[1−3] An ideal solution is to selectively hydrogenate the trace amount of acetylene to ethylene. Pd nanoparticles (NPs) are so far regarded as the most efficient catalyst for such catalytic reaction.[1] However, pure Pd metal catalysts possess very poor selectivity for high acetylene conversion in the presence of ethylene.[4,5] For this reason, pure Pd metal was modified with surface modifiers, such as lead acetate or quinoline (e.g., those in Lindlar catalyst) to enhance the selectivity of acetylene hydrogenation. However, these catalysts were usually toxic, and large amounts of environmental pollutants (e.g., Pb or sulfur containing compounds) could be produced as byproducts.[6−9] Other ways to enhance the selectivity included depositing a second metal or metal oxide on Pd nanoparticles or fabricating intermetallic compounds.[3,10−13] These methods were often regarded as "site-isolative" structural modification (and thus electronic modification) of the active Pd component.[14] However, the complexity in catalyst preparation and relatively low performance of these bimetallic Pd catalysts keep driving researchers to search for more efficient and sustainable new catalysts.

It has been revealed that the hydrogen atoms tend to diffuse into the subsurface region of Pd nanoparticles/clusters during hydrogenation reactions.[15−17] These subsurface hydrogen atoms called β-hydride or β-H are much more active than adsorbed surface hydrogen species, which caused the overhydrogenation of alkynes and thus lowered the selectivity toward alkene.[16] Interestingly, some studies found that the formation of palladium carbide (PdC_x) during alkyne hydrogenation had a decisive influence on catalytic selectivity.[3,18,19] Carbon atoms incorporated into top Pd layers could reduce β-H's rate of diffusion (to catalytic surfaces) and hinder its participation in the catalytic process.[15] Meanwhile, carbon atoms dissolved in the top Pd layers were likely to modify

Received: July 16, 2018
Published: September 24, 2018

DOI: 10.1021/jacs.8b07476
J. Am. Chem. Soc. XXXX, XXX, XXX−XXX

surface electronic structure of Pd,[15] leading to favored partial hydrogenation. Thus, it is vital to design a catalyst free of β-hydride but with good activity and a suitable desorption barrier and hydrogenation barrier of ethylene.

Here, we report a strategy to prepare Pd catalyst that consists of isolated Pd atoms anchoring onto the defective ND@G nanocarbon support (Pd_1/ND@G). Our catalyst showed high activity and excellent selectivity for acetylene hydrogenation. We found that the Pd species in the Pd_1/ND@G interact strongly with the support, becoming embedded in the graphene defects through bonding with C atoms. The unique structure of the atomically dispersed Pd catalyst rendering the easy desorption of the surface C_2H_4* species, which is the key for the excellent selectivity, in sharp contrast with Pd nanocluster catalysts.

The ND@G carbon material used here contains a thin graphene shell with abundant defects formed during the annealing of nanodiamonds.[20] The role of nanodiamond is that it is a perfect substrate for the grown of highly defective few-layer graphene outersheet with curvature, which is pivotal to preparation of Pd catalysts.[21] High-resolution transmission electron microscopy (HRTEM) images, Raman spectra and XPS measurements (see Figure S1 and S2) revealed that ND@G was covered with a defective graphene shell. By modulating the loading amount of Pd on graphitic carbon shell, we could change the dispersion of Pd to make two different types of catalysts: Pd_1/ND@G (0.11 wt %) and Pd_n/ND@G (0.87 wt %) where Pd_n denotes Pd clusters. The detailed structural information on the catalysts is shown in Table S1. From XRD profiles (see Figure S3), it is clear that no diffraction associated with bulk Pd was observed on both samples, indicating that Pd species were highly dispersed over the surface of ND@G composite.

The aberration-corrected high-angle annular dark-field scanning transmission electron microscopy (HAADF-STEM) was used to study the dispersion of Pd on ND@G (see Figure 1). For Pd_n/ND@G, the sample was found with Pd clusters, together with some amount of atomically dispersed Pd species. Instead, for Pd_1/ND@G catalyst, no Pd nanoclusters and nanoparticles were observed, and the Pd element existed exclusively as atomically dispersed Pd species on ND@G. Significantly, this is a very simple new method to prepare the atomically dispersed Pd catalyst.[22,23]

To further investigate the distinct structure of Pd species, we used X-ray adsorption fine structure (XAFS) spectra to study the Pd_1/ND@G and Pd_n/ND@G, together with two reference samples: Pd foil and PdO. From the X-ray absorption near-edge structure (XANES) spectroscopy (see Figure 2a), the near-edge feature of Pd_1/ND@G or Pd_n/ND@G shifted to higher valence state compared to that of Pd foil, indicating the existence of slightly positively charged Pd species. More interestingly, the absorption of Pd_1/ND@G is located between that of Pd_n/ND@G and PdO, suggesting that the atomically dispersed Pd species has stronger interaction with ND@G than Pd in Pd_n/ND@G. As shown in Figure 2b, the Fourier-transformed (FT) k^2-weighted extended X-ray absorption fine structure (EXAFS) provided key evidence of the coordination environments of Pd atoms anchored on ND@G. For Pd_1/ND@G, the only distinct peak observed at 1.5 Å corresponds to the first coordination shell of Pd in a bonding configuration of Pd−C or Pd−O.[23] In contrast, for Pd_n/ND@G, besides the peak of Pd−C/O, an appreciable peak at about 2.4 Å can be ascribed to first shell Pd−Pd coordination, indicating the

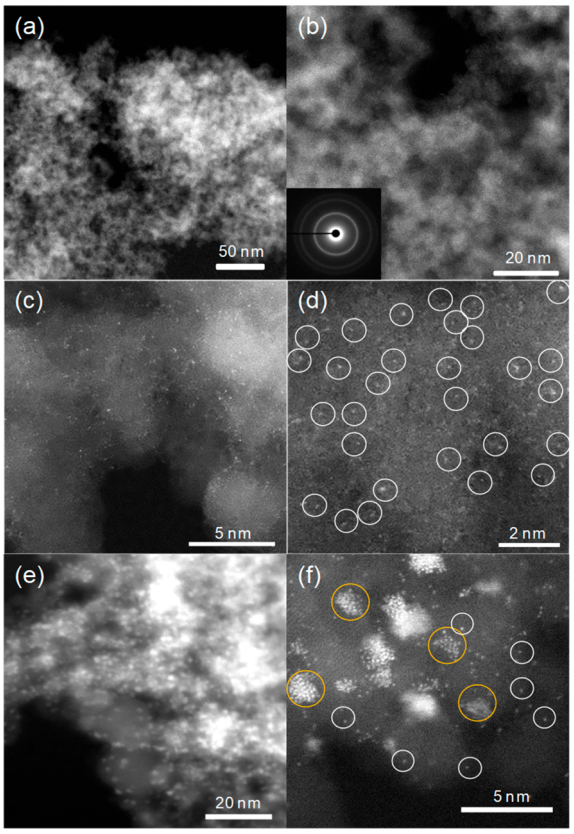

Figure 1. HAADF-STEM images of Pd_1/ND@G at low (a, b) and high (c, d) magnifications; STEM (e) and HAADF-STEM (f) images of Pd_n/ND@G. (The inset in image b is a diamonds diffraction rings image; atomically dispersed Pd atoms in image d are highlighted by the white circles; and Pd nanoclusters in image f are highlighted by the yellow circles.)

formation of Pd nanoclusters. Wavelet transform (WT) of Pd L_3-edge EXAFS oscillations further display visually the atomic dispersion of Pd throughout the whole catalyst. In Figures 2c,d, WT plots of Pd_1/ND@G and Pd_n/ND@G showed one maximum near 1.5 Å, which is associated with the Pd−C/O contribution. However, as shown in Figure 2d, another maximum can be observed at 2.4 Å for Pd clusters, which can be attributed to the existence of Pd−Pd scattering. These results further confirm the formation of Pd nanoclusters. The least-squares EXAFS fitting curves of Pd_1/ND@G and Pd_n/ND@G are shown in Figure S4, and the corresponding structure parameters are listed in Table S2. The coordination number of the Pd with surrounding C/O atoms on Pd_1/ND@G is about 2.6, and the mean bond length of Pd−C/O is 2.04 Å. The interatomic bond length decreases as the Pd−Pd coordination number decreases, which is in accordance with previous reports.[6,22,24−27] To further unravel the local structure of atomically dispersed Pd species, we investigated different bonding models of Pd-$(C/O)_x$ motif on ND@G through the calculations at the level of density functional theory (DFT). Considering the practical situation in which H_2 is presented and participated in the reaction, it is highly possible that Pd−O was not stable on ND@G, as oxygen can be easily captured by H_2 to form H_2O (see Table S8−S10). Based on the above analysis, the local atomic structure around Pd was constructed (Figure 2e). The isolated Pd atom was anchored through three carbon atoms over the defective sites of graphene, forming a

DOI: 10.1021/jacs.8b07476
J. Am. Chem. Soc. XXXX, XXX, XXX−XXX

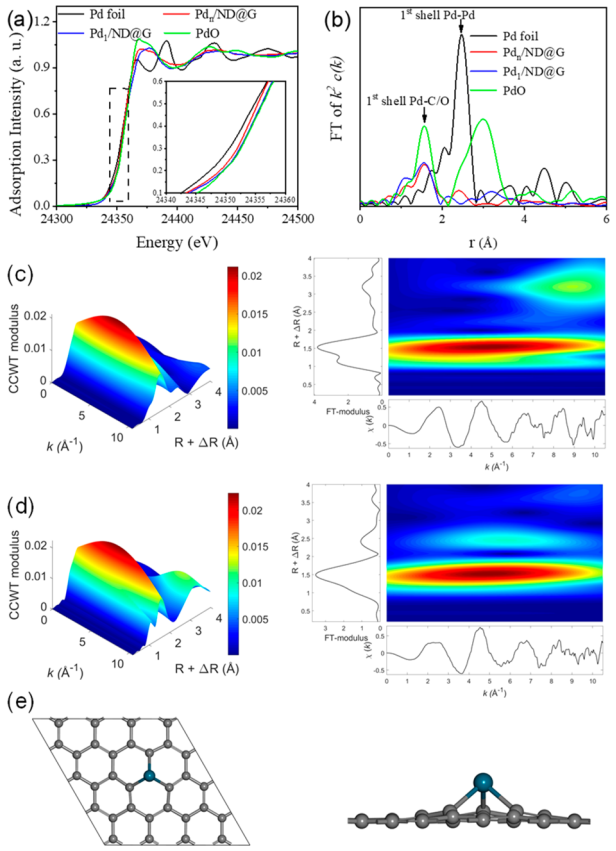

Figure 2. Pd K-edge XANES profiles (a) and EXAFS spectra (b) for Pd$_1$/ND@G and Pd$_n$/ND@G (inset: expansion of the highlighted region); WT analysis of Pd$_1$/ND@G (c) and Pd$_n$/ND@G (d); and the optimized structure of Pd atom embedded into graphene from top (left) and side (right) views (e). Color code: Pd (blue) and C (dark).

pyramidal geometry through covalent bond between Pd and carbon atoms.

Catalytic performance of Pd$_1$/ND@G was evaluated and compared to Pd$_n$/ND@G for semihydrogenation of acetylene, as shown in Figure 3. The conversion of acetylene as a function of temperature over those catalysts is shown in Figure 3a. For pure ND@G support, no hydrogenation products were detected at a series of reaction temperatures, indicating that the support itself was inert in such reaction. For Pd$_n$/ND@G, it exhibited extremely high catalytic activity even at room temperature. However, the selectivity of ethylene (see the SI for the calculation method of selectivity) was −450% over Pd$_n$/ND@G. This means, when the conversion of acetylene reached at full, the selectivity of ethylene decreased to negative value, as shown in Figure 3b. This demonstrated that a large amount of ethylene in the feed was converted to ethane, which produced low valued product while wasting the raw ethylene. Significantly, by isolating Pd atoms on ND@G, Pd$_1$/ND@G manifested robust catalytic activity and remarkably higher selectivity toward ethylene than Pd$_n$/ND@G (see Figure 3b). The selectivity of Pd$_1$/ND@G toward ethylene was >90% even when the conversion of acetylene reached 100% at 180 °C. The turnover frequency (TOFs) of Pd$_1$/ND@G is as high as 0.064 s^{-1}, surpassing the atomically dispersed Pd catalysts reported so far (see Figure S6). The stability of Pd$_1$/ND@G catalyst was evaluated. As shown in Figure 3c, the conversion and selectivity at 180 °C over Pd$_1$/ND@G kept steady at 100% and 90% respectively for at least 30 h. Notably, even for

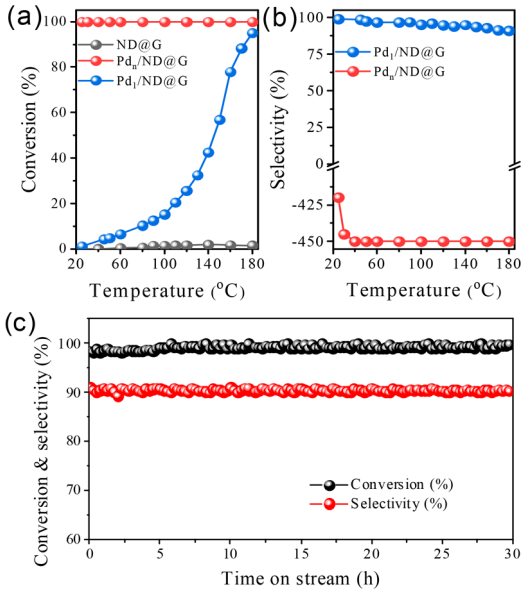

Figure 3. Conversion (a) and selectivity (b) as a function of temperature for acetylene hydrogenation over Pd$_n$/ND@G and Pd$_1$/ND@G catalysts; and durability test on Pd$_1$/ND@G at 180 °C for 30 h (c). (Reaction conditions: 1% C_2H_2, 10% H_2, 20% C_2H_4 gas mix balanced with He; GHSV = 60000 h^{-1}.)

catalyst after 30 h in reaction, no visible metallic atom aggregation was observed by HAADF-STEM (see Figure S5). This observation suggests that the substrates anchoring through Pd−C binding can effectively create high-performance catalyst, and Pd$_1$/ND@G is steady against deactivation and sintering during the reaction. Besides, Pd$_1$/ND@G avoid oligomerization of acetylene and coking, which accounts for the excellent stability and is in accordance with previous reports.[28]

The lack of β-H reservoir in the Pd$_1$/ND@G catalyst (compared to conventional Pd catalyst and Pd$_n$/ND@G) could suppress the opportunity of further hydrogenation of ethylene to ethane, due to the control of reaction kinetics. This is one of the main reasons for the excellent selectivity of Pd$_1$/ND@G. Why does the atomically dispersed Pd catalyst have such high selectivity for acetylene hydrogenation? To resolve this puzzle, we built the model of atomically dispersed Pd on defective graphene (termed as Pd$_1$@Gr) according to the deduced catalyst structures in experiments (other candidate configurations are described in the Supporting Information), and studied the reaction mechanism by quantum chemistry simulation at the DFT level.[29] As shown in Figure 4, acetylene gas molecule preferentially adsorbed on Pd atom of Pd$_1$@Gr. The adsorption energy of acetylene on Pd atom of Pd$_1$@Gr (−0.61 eV, Table S13) is much weaker than that on the Pd(111) surface (−1.79 eV).[30] Then, the molecular hydrogen undergoes heterolytic dissociation (C), leaving one of the hydrogen atoms bound to a C atom and the other one to a Pd atom. This step is endothermic by 0.44 eV with an energy barrier of 1.10 eV (from B to C). The following reaction to vinyl molecule is free of barrier and is exothermic by −1.35 eV (from C to D). From vinyl molecule to adsorbed ethylene species, the process experiences further hydrogenation with an energy barrier of 0.85 eV (TS3 shown in Table S13 and Figure S8) and is exothermic by −1.30 eV (from D to F). Although the simulated elementary steps for further hydrogenation of

DOI: 10.1021/jacs.8b07476
J. Am. Chem. Soc. XXXX, XXX, XXX−XXX

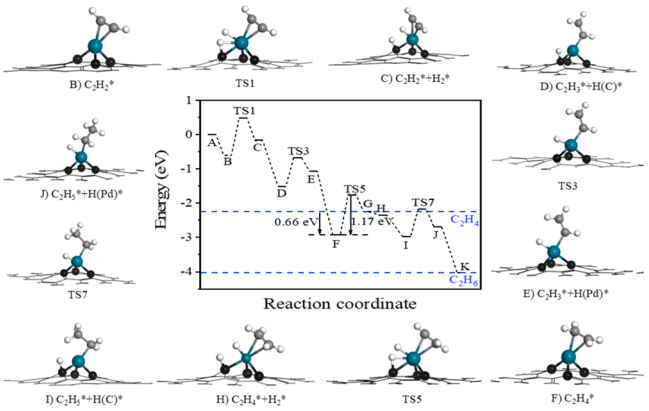

Figure 4. Energy profile of acetylene hydrogenation on the Pd_1/ND@G catalyst. Color code: Pd (blue), C in graphene (black), C in reactant/intermediates/product (gray), and H (white).

ethylene to ethane are still thermodynamically exothermic on isolated Pd active sites, the barrier of further hydrogenation of adsorbed C_2H_4 intermediate to ethane (1.17 eV) is much higher than the desorption energy of surface C_2H_4 species to the gas phase (0.66 eV). The high selectivity of acetylene hydrogenation reaction here is due to the competition of ethylene desorption at the catalytic active sites of Pd_1/ND@G.

In summary, we report a new method to prepare an atomically dispersed metal catalyst (in this case, Pd_1/ND@G), which exhibited remarkably high selectivity (90%) for the hydrogenation of acetylene to ethylene with a 100% conversion. The suppression of further hydrogenation of ethylene to ethane is linked to the lack of unselective subsurface hydrogen and the presence of an energetic favored path for the aimed product, ethylene, desorption in the Pd_1/ND@G catalyst. This catalyst design strategy offers a simple method to prepare atomically dispersed metal catalysts, paving the way for rational design of highly selective catalysts.

■ ASSOCIATED CONTENT

Supporting Information

The Supporting Information is available free of charge on the ACS Publications website at DOI: 10.1021/jacs.8b07476.

Detailed experimental procedures, characterization methods and additional tables and figures (PDF)

■ AUTHOR INFORMATION

Corresponding Authors

*liuhy@imr.ac.cn

*dma@pku.edu.cn

ORCID

Xiangbin Cai: 0000-0002-8634-3834

Pengju Ren: 0000-0003-3752-1638

Xiaodong Wen: 0000-0001-5626-8581

Ning Wang: 0000-0002-4902-5589

Hongyang Liu: 0000-0003-2977-2867

Ding Ma: 0000-0002-3341-2998

Author Contributions

#These authors contributed equally to this work.

Notes

The authors declare no competing financial interest.

■ ACKNOWLEDGMENTS

This work was supported by the Ministry of Science and Technology (2016YFA0204100, 2017YFB0602200), the National Natural Science Foundation of China (21573254, 91545110, 21725301, 91645115, 21473003 and 21821004), the Youth Innovation Promotion Association, Chinese Academy of Science (CAS). N.W. hereby acknowledges the funding support from the Research Grants Council of Hong Kong (Project Nos. C6021-14E and 16306818). The XAS experiments were conducted in Shanghai Synchrotron Radiation Facility (SSRF).

■ REFERENCES

(1) Studt, F.; Abild-Pedersen, F.; Bligaard, T.; Sørensen, R. Z.; Christensen, C. H.; Nørskov, J. K. *Science* **2008**, *320*, 1320.

(2) Chan, C. W. A.; Mahadi, A. H.; Li, M. M.-J.; Corbos, E. C.; Tang, C.; Jones, G.; Kuo, W. C. H.; Cookson, J.; Brown, C. M.; Bishop, P. T.; Tsang, S. C. E. *Nat. Commun.* **2014**, *5*, 5787.

(3) Teschner, D.; Révay, Z.; Borsodi, J.; Hävecker, M.; Knop-Gericke, A.; Schlögl, R.; Jackson, S. D.; Torres, D.; Sautet, P.; Milroy, D. *Angew. Chem., Int. Ed.* **2008**, *47*, 9274.

(4) Vilé, G.; Albani, D.; Almora-Barrios, N.; López, N.; Pérez-Ramírez, J. *ChemCatChem* **2016**, *8*, 21.

(5) Liu, Y.; Liu, X.; Feng, Q.; He, D.; Zhang, L.; Lian, C.; Shen, R.; Zhao, G.; Ji, Y.; Wang, D.; Zhou, G.; Li, Y. *Adv. Mater.* **2016**, *28*, 4747.

(6) Vilé, G.; Albani, D.; Nachtegaal, M.; Chen, Z.; Dontsova, D.; Antonietti, M.; López, N.; Pérez-Ramírez, J. *Angew. Chem., Int. Ed.* **2015**, *54*, 11265.

(7) Armbrüster, M.; Kovnir, K.; Behrens, M.; Teschner, D.; Grin, Y.; Schlögl, R. *J. Am. Chem. Soc.* **2010**, *132*, 14745.

(8) Hu, T.-L.; Wang, H.; Li, B.; Krishna, R.; Wu, H.; Zhou, W.; Zhao, Y.; Han, Y.; Wang, X.; Zhu, W.; Yao, Z.; Xiang, S.; Chen, B. *Nat. Commun.* **2015**, *6*, 7328.

(9) López, N.; Vargas-Fuentes, C. *Chem. Commun.* **2012**, *48*, 1379.

(10) Zhou, H.; Yang, X.; Li, L.; Liu, X.; Huang, Y.; Pan, X.; Wang, A.; Li, J.; Zhang, T. *ACS Catal.* **2016**, *6*, 1054.

(11) Feng, Q.; Zhao, S.; Wang, Y.; Dong, J.; Chen, W.; He, D.; Wang, D.; Yang, J.; Zhu, Y.; Zhu, H.; Gu, L.; Li, Z.; Liu, Y.; Yu, R.; Li, J.; Li, Y. *J. Am. Chem. Soc.* **2017**, *139*, 7294.

(12) Xiang, S.-C.; Zhang, Z.; Zhao, C.-G.; Hong, K.; Zhao, X.; Ding, D.-R.; Xie, M.-H.; Wu, C.-D.; Das, M. C.; Gill, R.; Thomas, K. M.; Chen, B. *Nat. Commun.* **2011**, *2*, 204.

(13) Vignola, E.; Steinmann, S. N.; Le Mapihan, K.; Vandegehuchte, B. D.; Curulla, D.; Sautet, P. *J. Phys. Chem. C* **2018**, *122*, 15456.

(14) Teschner, D.; Borsodi, J.; Wootsch, A.; Révay, Z.; Hävecker, M.; Knop-Gericke, A.; Jackson, S. D.; Schlögl, R. *Science* **2008**, *320*, 86.

(15) Tew, M. W.; Janousch, M.; Huthwelker, T.; van Bokhoven, J. A. *J. Catal.* **2011**, *283*, 45.

(16) García-Mota, M.; Bridier, B.; Pérez-Ramírez, J.; López, N. *J. Catal.* **2010**, *273*, 92.

(17) Ludwig, W.; Savara, A.; Madix, R. J.; Schauermann, S.; Freund, H.-J. *J. Phys. Chem. C* **2012**, *116*, 3539.

(18) Wilde, M.; Fukutani, K.; Ludwig, W.; Brandt, B.; Fischer, J. H.; Schauermann, S.; Freund, H. *Angew. Chem., Int. Ed.* **2008**, *47*, 9289.

(19) Neyman, K. M.; Schauermann, S. *Angew. Chem., Int. Ed.* **2010**, *49*, 4743.

(20) Liu, J.; Yue, Y.; Liu, H.; Da, Z.; Liu, C.; Ma, A.; Rong, J.; Su, D.; Bao, X.; Zheng, H. *ACS Catal.* **2017**, *7*, 3349.

(21) Huang, F.; Liu, H.; Su, D. *Sci. China Mater.* **2017**, *60*, 1149.

(22) Chen, Z.; Vorobyeva, E.; Mitchell, S.; Fako, E.; Ortuño, M. A.; López, N.; Collins, S. M.; Midgley, P. A.; Richard, S.; Vilé, G.; Pérez-Ramírez, J. *Nat. Nanotechnol.* **2018**, *13*, 702.

(23) Yan, H.; Cheng, H.; Yi, H.; Lin, Y.; Yao, T.; Wang, C.; Li, J.; Wei, S.; Lu, J. *J. Am. Chem. Soc.* **2015**, *137*, 10484.

DOI: 10.1021/jacs.8b07476
J. Am. Chem. Soc. XXXX, XXX, XXX−XXX

(24) Yao, S.; Zhang, X.; Zhou, W.; Gao, R.; Xu, W.; Ye, Y.; Lin, L.; Wen, X.; Chen, B.; Crumlin, E.; Guo, J.; Zuo, Z.; Li, W.; Xie, J.; Lu, L.; Kiely, C. J.; Gu, L.; Shi, C.; Rodriguez, J. A.; Liu, P.; Ma, D. *Science* **2017**, *357*, 389.
(25) Qiao, B.; Wang, A.; Yang, X.; Allard, L. F.; Jiang, Z.; Cui, Y.; Liu, J.; Li, J.; Zhang, T. *Nat. Chem.* **2011**, *3*, 634.
(26) Lin, L.; Zhou, W.; Gao, R.; Yao, S.; Zhang, X.; Xu, W.; Zheng, S.; Jiang, Z.; Yu, Q.; Li, Y.-W.; Shi, C.; Wen, X.-D.; Ma, D. *Nature* **2017**, *544*, 80.
(27) Jones, J.; Xiong, H.; DeLaRiva, A. T.; Peterson, E. J.; Pham, H.; Challa, S. R.; Qi, G.; Oh, S.; Wiebenga, M. H.; Pereira Hernández, X. I.; Wang, Y.; Datye, A. K. *Science* **2016**, *353*, 150.
(28) Vignola, E.; Steinmann, S. N.; Al Farra, A.; Vandegehuchte, B. D.; Curulla, D.; Sautet, P. *ACS Catal.* **2018**, *8*, 1662.
(29) Albani, D.; Shahrokhi, M.; Chen, Z.; Mitchell, S.; Hauert, R.; López, N.; Pérez-Ramírez, J. *Nat. Commun.* **2018**, *9*, 2634.
(30) Sheth, P. A.; Neurock, M.; Smith, C. M. *J. Phys. Chem. B* **2003**, *107*, 2009.

DOI: 10.1021/jacs.8b07476
J. Am. Chem. Soc. XXXX, XXX, XXX−XXX